

# Influence of Chemical Reaction and Heat Generation/Absorption on MHD Free Convective Heat and Mass Transfer Flow along an Inclined Stretching Sheet Considering Dufour and Soret Effects

Md. Shariful Alam<sup>1</sup> and Md. Shirazul Hoque Mollah<sup>2</sup>

<sup>1</sup>Department of Mathematics, Jagannath University, Dhaka-1100, Bangladesh

Email: msalam631@yahoo.com

<sup>2</sup>Department of Mathematics, Dhaka University of Engineering and Technology (DUET), Gazipur,

Gazipur-1700, Bangladesh, Email: mollah123@yahoo.com

**Abstract**-In this paper, the influence of chemical reaction and heat generation or absorption on MHD free convection and mass transfer flow of a viscous, incompressible and electrically conducting fluid over an inclined stretching sheet is investigated numerically, by taking into account the Dufour and Soret effects. The non-linear boundary layer equations with the boundary conditions are transferred by a similarity transformation into a system of non-linear ordinary differential equations. These non-linear and self-similar ordinary differential equations are solved numerically by using a sixth-order Runge-Kutta integration scheme with the shooting method. Comparison with previous published work was performed and excellent agreement is obtained. The effects of various parameters on the velocity, temperature and concentration profiles as well as the local skin-friction coefficient, heat and mass transfer rate from the stretching sheet to the surrounding fluid are presented graphically and in tabulated form for a hydrogen-air mixture. The numerical results showed that chemical reaction parameter  $K$  and the order of reaction  $n$  play a crucial role in the solutions.

**Keywords:** Chemical reaction, Dufour effect, Soret effect, Shooting method.

## 1. INTRODUCTION

The continuous surface heat and mass transfer problem has many practical applications in electro-chemistry and polymer processing. In light of these applications, Char [1] analyzed heat and mass transfer in a hydro magnetic flow of the visco-elastic fluid over a stretching sheet. Acharya et al. [2] studied heat and mass transfer over an accelerating surface with heat source in the presence of suction and blowing. Khan et al. [3] investigated visco-elastic MHD flow; heat and mass transfer over a porous stretching sheet with dissipation of energy and stress work. Recently

Sanjayanand and Khan [4] studied heat and mass transfer in a visco-elastic boundary layer flow over an exponentially stretching sheet.

However in some industrial processes involving heat and mass transfer over a moving surface the diffusion species can be generated or absorbed due to some kind of chemical reaction with the ambient fluid. This generation or absorption of species can affect the flow and accordingly the properties and quality of the final product. Fan et al. [5] studied similarity solution of mixed convection with diffusion and chemical reaction over a horizontal moving plate. Takhar et al. [6] analyzed the flow and mass transfer on a stretching sheet with chemically reactive species in the presence of a magnetic field. Effect of the chemical reaction and injection on flow characteristics in an unsteady upward motion of an isothermal plate was studied by Muthucumaraswamy and Ganesan [7]. Chamkha [8] investigated the effect of chemical reaction on MHD flow of a uniformly stretched vertical permeable surface in the presence of heat generation or absorption. Kandasamy et al. [9] studied the effects of chemical reaction; heat and mass transfer along a wedge with heat source and concentration in the presence of suction or injection.

In the previous papers, the diffusion-thermo (Dufour) and thermal-diffusion (Soret) terms have been neglected from the energy and concentration equations respectively. Thermal diffusion, also called thermodiffusion or Soret effect corresponds to species differentiation developing in an initial homogeneous mixture submitted to a thermal gradient. The energy flux caused by a composition gradient is called Dufour or diffusion-thermo effect. These effects are considered as second-order phenomenon, on the basis that they are of smaller order of magnitude than the effects described by Fourier's and Fick's laws, but they may become significant in areas such geosciences or hydrology. Kafoussias and Williams [10] studied the thermal-diffusion and diffusion-thermo effects on mixed free-forced convective and mass transfer

boundary layer flow with temperature dependent viscosity. Anghel et al. [11] investigated the Dufour and Soret effects on free convection boundary layer over a vertical surface embedded in a porous medium. Eldabe et al. [12] investigated the thermal-diffusion and diffusion-thermo effects on mixed free-forced convection and mass transfer boundary layer flow for non-Newtonian fluid with temperature dependent viscosity. Salem [13] analyzed thermal-diffusion and diffusion-thermo effects on convective heat and mass transfer in a visco-elastic fluid flow through a porous medium over a stretching sheet. Alam et al. [14] investigated the Dufour and Soret effects on unsteady MHD free convection and mass transfer flow past a vertical porous plate in a porous medium. Postelnicu [15] studied the influence of chemical reaction on heat and mass transfer by natural convection from vertical surfaces in porous media considering Soret and Dufour effects. The order of the reaction in that paper was taken as  $n = 1, 2$  and  $3$ .

Therefore our aim of the present paper is to investigate the effect of  $n$ th order chemical reaction and heat generation or absorption on MHD free convective flow with heat and mass transfer over an inclined permeable stretching sheet under the influence of Dufour and Soret effects with variable wall temperature and concentration.

## 2. MATHEMATICAL ANALYSIS

We consider a steady two-dimensional; laminar MHD free convective heat and mass transfer flow of a viscous and incompressible fluid along a linearly stretching semi-infinite sheet that is inclined from the vertical with an acute angle  $\alpha$ . The surface is assumed to be permeable and moving with velocity,  $u_w(x) = bx$  (where  $b$  is constant called stretching rate). Fluid suction or injection is imposed at the stretching surface. The  $x$ -axis runs along the stretching surface in the direction of motion with the slot as the origin and the  $y$ -axis is measured normally from the sheet to the fluid. A magnetic field of uniform strength  $B_0$  is applied normal to the sheet in the  $y$ -direction, which produces magnetic effect in the  $x$ -direction. A heat source or sink is placed within the flow to allow for possible heat generation or absorption effects. The fluid is assumed to be Newtonian, electrically conducting and heat generating or absorbing. We further assume that there exists a homogeneous  $n$ th order chemical reaction between the fluid and species concentration.

Under the above assumption and along with Boussinesq's and boundary layer approximation, the governing equations describing the conservation of

mass, momentum, energy and concentration respectively are as follows:

$$\frac{\partial u}{\partial x} + \frac{\partial v}{\partial y} = 0, \tag{1}$$

$$u \frac{\partial u}{\partial x} + v \frac{\partial u}{\partial y} = \nu \frac{\partial^2 u}{\partial y^2} + g\beta(T - T_\infty) \cos \alpha + g\beta^*(C - C_\infty) \cos \alpha - \frac{\sigma B_0^2}{\rho} u, \tag{2}$$

$$u \frac{\partial T}{\partial x} + v \frac{\partial T}{\partial y} = \frac{k}{\rho c_p} \frac{\partial^2 T}{\partial y^2} + \frac{D_m k_T}{c_s c_p} \frac{\partial^2 C}{\partial y^2} + \frac{Q_0}{\rho c_p} (T - T_\infty), \tag{3}$$

$$u \frac{\partial C}{\partial x} + v \frac{\partial C}{\partial y} = D_m \frac{\partial^2 C}{\partial y^2} + \frac{D_m k_T}{T_m} \frac{\partial^2 T}{\partial y^2} - K_1 (C - C_\infty)^n. \tag{4}$$

The boundary conditions suggested by the physics of the problem are:

$$u = u_w(x) = bx, v = \pm v_w(x), T_w - T_\infty = A_1 x^r, C_w - C_\infty = A_2 x^r \quad \text{at } y = 0, \tag{5a}$$

$$u = 0, T = T_\infty, C = C_\infty \quad \text{as } y \rightarrow \infty, \tag{5b}$$

where  $b$  is a constant called stretching rate and  $A_1, A_2$  are proportionality constants and  $v_w(x)$  represents the permeability of the porous surface where its sign indicates suction ( $< 0$ ) or injection ( $> 0$ ). Here  $r$  is the temperature parameter and for  $r = 0$ , the thermal boundary conditions become isothermal.

Now, with the help of the similarity variables (see also Acharya et al. [2]):

$$\left. \begin{aligned} \psi &= (\nu b)^{1/2} x f(\eta), \eta = (b/\nu)^{1/2} y, \\ \theta(\eta) &= \frac{T - T_\infty}{T_w - T_\infty}, \phi(\eta) = \frac{C - C_\infty}{C_w - C_\infty}. \end{aligned} \right\} \tag{6}$$

Eqs. (2)-(4) become

$$f''' + ff'' - (f')^2 + g_s \theta \cos \alpha + g_c \phi \cos \alpha - Mf' = 0, \tag{7}$$

$$\theta'' - r \text{Pr} f'\theta + \text{Pr} f\theta' + \text{Pr} Df\phi'' + \text{Pr} Q\theta = 0, \tag{8}$$

$$\phi'' - r \text{Sc} f'\phi + \text{Sc} f\phi' + \text{Sc} S r \theta'' - \text{Sc} K \phi^n = 0. \tag{9}$$

The boundary conditions (5) then turn into

$$f = f_w, f' = 1, \theta = 1, \phi = 1 \quad \text{at } \eta = 0, \tag{10a}$$

$$f' = 0, \theta = 0, \phi = 0 \quad \text{as } \eta \rightarrow \infty, \tag{10b}$$

where  $f_w = -v_w / (b\nu)^{1/2}$  is the dimensionless wall mass transfer coefficient such that  $f_w > 0$  indicates wall suction and  $f_w < 0$  indicates wall injection.

The dimensionless parameters introduced in the above equations are defined as follows:

$M = \frac{\sigma B_0^2 x}{\rho u_w(x)}$  is the local Magnetic field parameter,

$Gr = \frac{g\beta(T_w - T_\infty)x^3}{\nu^2}$  is the local Grashof number,

$Gm = \frac{g\beta^*(C_w - C_\infty)x^3}{\nu^2}$  is the local modified Grashof number,

$Re_x = \frac{u_w(x)x}{\nu}$  is the local Reynolds number,

$g_s = \frac{Gr}{Re_x^2}$  is the temperature buoyancy parameter,

$g_c = \frac{Gm}{Re_x^2}$  is the mass buoyancy parameter,

$Pr = \frac{\nu\rho c_p}{k}$  is the Prandtl number,

$Df = \frac{D_m k_T (C_w - C_\infty)}{\nu c_s c_p (T_w - T_\infty)}$  is the Dufour number,

$Sr = \frac{D_m (T_w - T_\infty)}{\nu (C_w - C_\infty) T_m}$  is the Soret number,

$Q = \frac{Q_0 x}{\rho c_p u_w(x)}$  is the heat generation/absorption parameter,

$Sc = \frac{\nu}{D_m}$  is the Schmidt number and

$K = \frac{K_l (C_w - C_\infty)^{n-1} x}{u_w(x)}$  is the chemical reaction parameter.

The parameters of engineering interest for the present problem are the local skin-friction coefficient, local Nusselt number and the local Sherwood number which are obtained from the following expressions:

$$\frac{1}{2} Cf_x (Re_x)^{\frac{1}{2}} = f''(0), \tag{11}$$

$$Nu_x (Re_x)^{\frac{1}{2}} = -\theta'(0), \tag{12}$$

$$Sh_x (Re_x)^{\frac{1}{2}} = -\phi'(0). \tag{13}$$

### 3. NUMERICAL COMPUTATION

The system of nonlinear ordinary differential equations (7)-(9) with the relevant boundary conditions (10) have been solved numerically by using sixth order Runge-Kutta integration scheme together with Nachtsheim-Swigert [16] shooting iteration technique (for detailed discussion of the method see Alam et al. [14]) with  $\alpha, g_s, g_c, M, Pr, Sc, r, f_w, Q, n, Df, Sr$  and  $K$  as prescribed parameters. A step size of  $\Delta\eta = 0.01$  was selected to be satisfactory for a convergence criterion of  $10^{-6}$  in all cases. The value of  $\eta_\infty$  was found to each iteration loop by the statement  $\eta_\infty = \eta_\infty + \Delta\eta$ . The maximum value of  $\eta_\infty$  to each group of parameters  $\alpha, g_s, g_c, M, Pr, Sc, r, f_w, Q, n, Df, Sr$  and  $K$  determined when the value of the unknown boundary conditions at  $\eta = 0$  not change to successful loop with error less than  $10^{-6}$ .

To assess the accuracy of the present numerical method, we have compared our local skin-friction coefficients ( $-f''(0)$ ) with Andersson et al. [17] in table-1 and we see that excellent agreement between the results exists. This leads credence to the present numerical code.

TABLE-1: Comparison of  $-f''(0)$  with Andersson et al. [17] for their Newtonian fluid case and for our  $\alpha = 90^\circ$  and  $f_w = g_s = g_c = 0$  case with different  $M$ .

$M$	Andersson et al. [17]	Present study
0.0	1.00	1.0000092
0.5	1.225	1.2247449
1.0	1.414	1.4142136
1.5	1.581	1.5811388
2.0	1.732	1.7320508

### 4. NUMERICAL RESULTS AND DISCUSSION

The results of the numerical computations are displayed graphically in Figs. 1-8 and in tables 2-3 for prescribed surface temperature. Results are obtained for  $Pr = 0.71$  (air),  $Sc = 0.22$  (hydrogen),  $g_s = 12$ ;  $g_c = 6$  (due to free convection problem) and various values of the magnetic field parameter  $M$ , suction parameter  $f_w$ , angle of inclination  $\alpha$  to vertical, surface temperature parameter  $r$ , Dufour number  $Df$ , Soret number  $Sr$ ,

chemical reaction parameter  $K$  and order of chemical reaction  $n$ .

Figs. 1(a)-(c) represent respectively, the dimensionless velocity, temperature and concentration for various values of the magnetic field parameter ( $M$ ). The presence of a magnetic field normal to the flow in an electrically conducting fluid produces a Lorentz force, which acts against the flow. This resistive force tends to slow down the flow and hence the fluid velocity decreases with the increase of the magnetic field parameter as observed in Fig. 1(a). From Fig. 1(b) we see that the temperature profiles increase with the increase of the magnetic field parameter, which implies that the applied magnetic field tends to heat the fluid, and thus reduces the heat transfer from the wall. In Fig. 1(c), the effect of an applied magnetic field is found to increase the concentration profiles, and hence increase the concentration boundary layer.

Representative velocity profiles for four typical angles of inclination ( $\alpha = 0^\circ, 30^\circ, 45^\circ$  and  $60^\circ$ ) are presented in Fig. 2(a). It is revealed from Fig. 2(a) that increasing the angle of inclination decreases the velocity. The fact is that as the angle of inclination increases the effect of the buoyancy force due to thermal diffusion decrease by a factor of  $\cos\alpha$ . Consequently the driving force to the fluid decreases as a result velocity profiles decrease. From Figs.2 (b)-(c) we also observe that both the thermal and concentration boundary layer thickness increase as the angle of inclination increases.

The effects of suction/injection parameter in the velocity field are shown in Fig. 3(a). It is found from this figure that the velocity profiles decrease monotonically with the increase of suction parameter indicating the usual fact that suction stabilizes the boundary layer growth. The effect of suction parameter on the temperature and concentration field is displayed in Figs. 3(b) and 3(c) respectively and we see that both the temperature and concentration decreases with the increase of suction parameter. Sucking decelerated fluid particles through the porous wall reduce the growth of the hydrodynamic, thermal and concentration boundary layers. Opposite phenomenon is observed for the case of fluid injection.

The effects of the surface temperature parameter  $r$  on the dimensionless velocity, temperature and concentration profiles are displayed in Figs. 4(a)-(c) respectively. From Fig. 4(a) it is seen that, the velocity gradient at the wall increases and hence the momentum boundary layer thickness decreases as  $r$  increases. Further more from Fig. 4(b) we can see that as  $r$  increases, the thermal boundary layer thickness decreases and the temperature gradient at the wall increases. This means a higher value of the heat transfer rate is associated with higher values of  $r$ . We also observe from Fig. 4(c) that the concentration

boundary layer thickness decreases as the exponent  $r$  increases.

Figs. 5(a)-(c) depict the influence of the dimensionless heat generation/absorption parameter  $Q$  on the fluid velocity, temperature and concentration profiles respectively. It is seen from Fig. 5(a) that when the heat is generated the buoyancy force increases, which induces the flow rate to increase giving, rise to the increase in the velocity profiles. From Fig. 5(b), we observe that when the value of the heat generation parameter  $Q$  increases, the temperature distribution also increases significantly which implies that owing to the presence of a heat source, the thermal state of the fluid increases causing the thermal boundary layer to increase. From Fig. 5(c) we also see that the concentration boundary layer thickness increases as the heat generation parameter  $Q$  increases. Opposite phenomenon is observed for the case of heat absorption.

The effects of chemical reaction parameter  $K$  on the velocity, temperature as well as concentration distributions are displayed in Figs. 6(a)-(c) respectively. It is observed from these figures that an increase in the chemical reaction parameter  $K$  leads to decrease the velocity and concentration profiles but leads to increase in the temperature profiles.

The influence of Soret number  $Sr$  and Dufour number  $Df$  on the velocity field are shown in Fig. 7(a). Quantitatively, when  $\eta = 1.0$  and  $Sr$  decreases from 2.0 to 1.5 (or  $Df$  increases from 0.03 to 0.04), there is 2.15% decrease in the velocity value whereas the corresponding decrease is 1.88% when  $Sr$  decreases from 1.0 to 0.5 (or  $Df$  increases from 0.06 to 0.12). From Fig. 7(b) when  $\eta = 1.0$  and  $Sr$  decreases from 2.0 to 1.5 (or  $Df$  increases from 0.03 to 0.04), there is 4.35% increase in the temperature, whereas the corresponding increase is 6.85% when  $Sr$  decreases from 1.0 to 0.5. In Fig. 7(c) when  $\eta = 1.0$  and  $Sr$  decreases from 2.0 to 1.5 (or  $Df$  increases from 0.03 to 0.04), there is 7.23% decrease in the concentration, whereas the corresponding decrease is 9.46% when  $Sr$  decreases from 1.0 to 0.5.

The effects of order of chemical reaction  $n$  on the velocity, temperature as well as concentration distributions are displayed in Figs. 8(a)-(c) respectively. It is observed from these figures that an increase in the chemical reaction order  $n$  leads to decrease the velocity and concentration profiles whereas the temperature profiles increases.

Finally, the effects of chemical reaction parameter, order of chemical reaction, Soret number and Dufour number on the local skin-friction coefficient, the local Nusselt number and the local Sherwood number are shown in Tables 2-3. The behavior of these parameters is self-evident from Tables 2-3 and hence they will not discuss any further due to brevity.

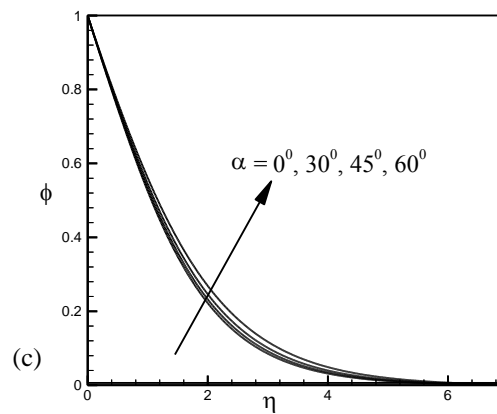
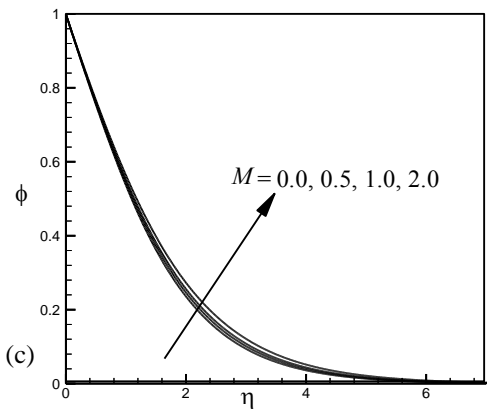
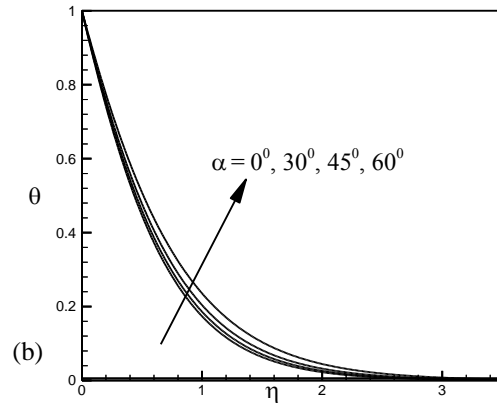
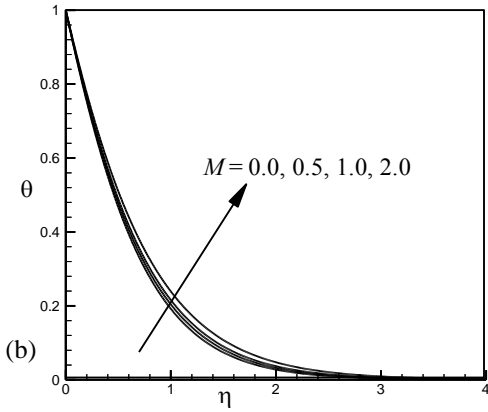
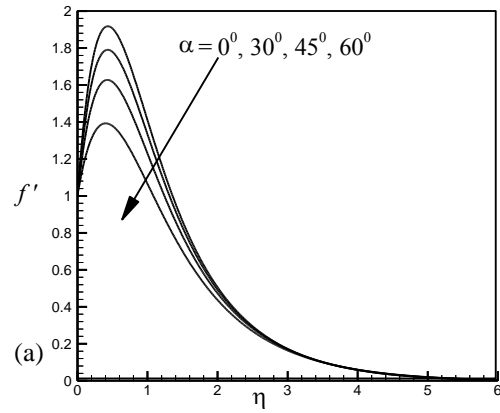
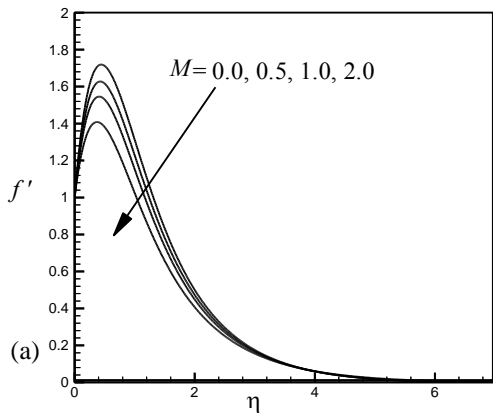


Fig.1: Variation of dimensionless (a) velocity, (b) temperature and (c) concentration profiles across the boundary layer for different values of  $M$ .

Fig.2: Variation of dimensionless (a) velocity, (b) temperature and (c) concentration profiles across the boundary layer for different values of  $\alpha$ .

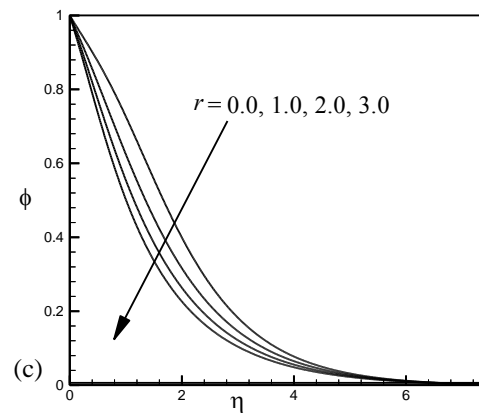
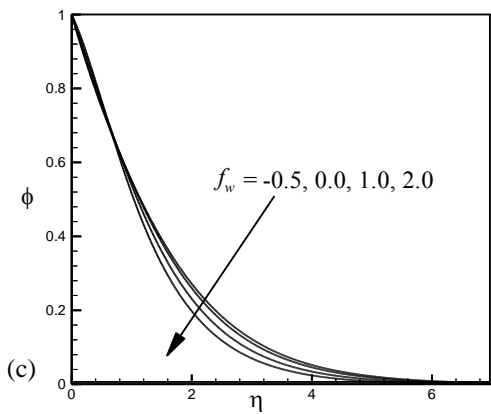
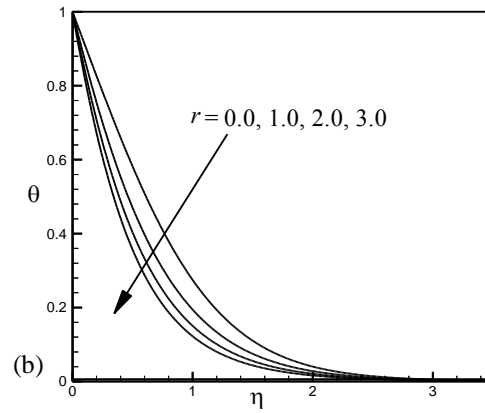
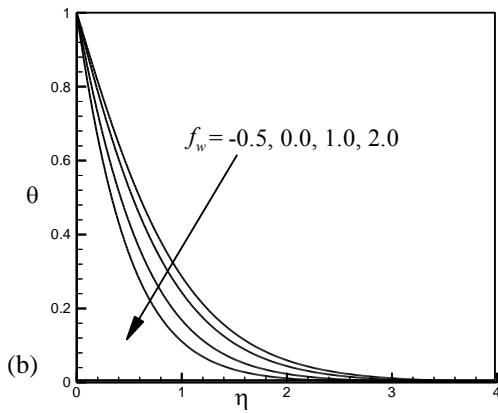
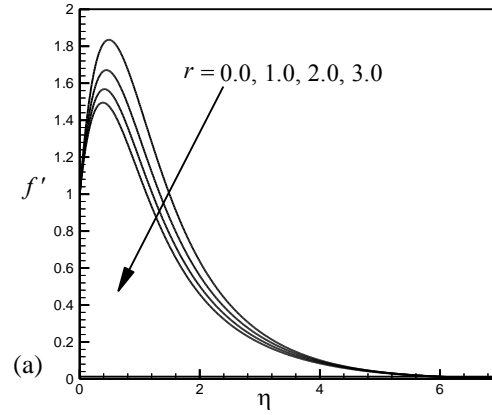
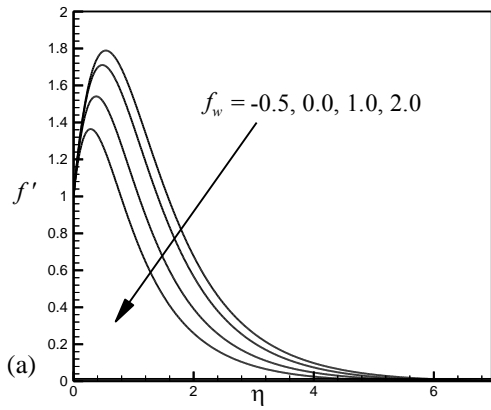


Fig.3: Variation of dimensionless (a) velocity, (b) temperature and (c) concentration profiles across the boundary layer for different values of  $f_w$ .

Fig. 4: Variation of dimensionless (a) velocity, (b) temperature and (c) concentration profiles across the boundary layer for different values of  $r$ .

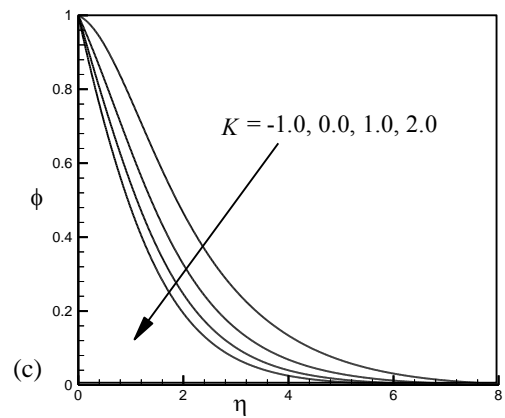
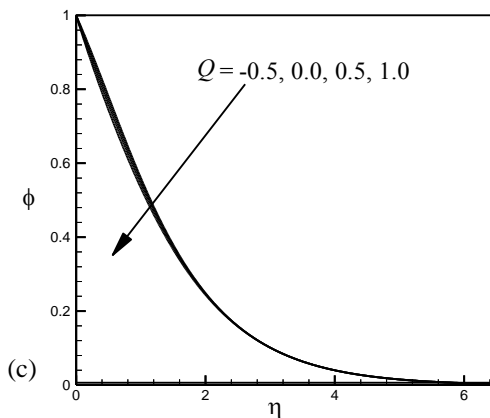
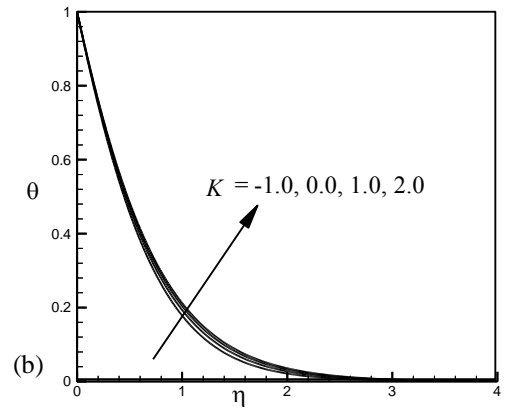
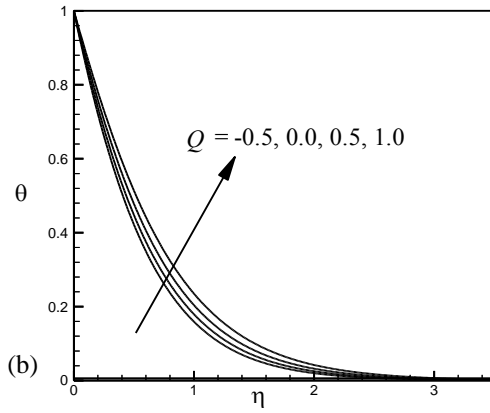
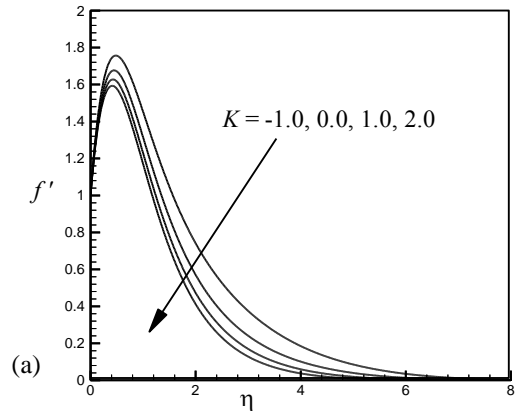
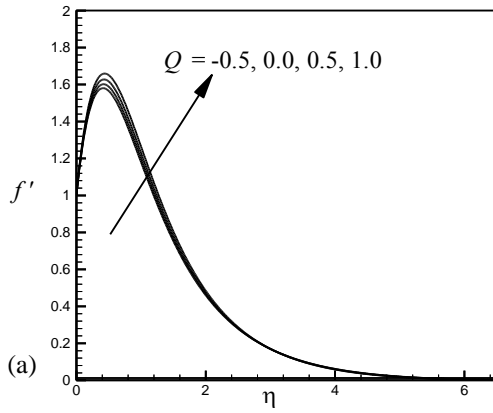


Fig.5: Variation of dimensionless (a) velocity, (b) temperature and (c) concentration profiles across the boundary layer for different values of  $Q$ .

Fig.6: Variation of dimensionless (a) velocity, (b) temperature and (c) concentration profiles across the boundary layer for different values of  $K$ .

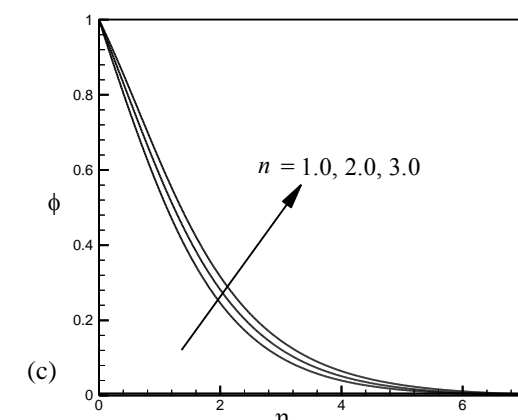
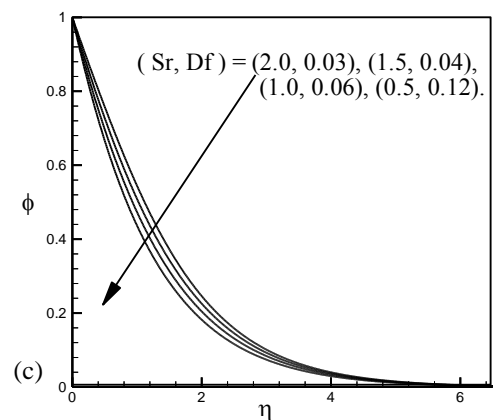
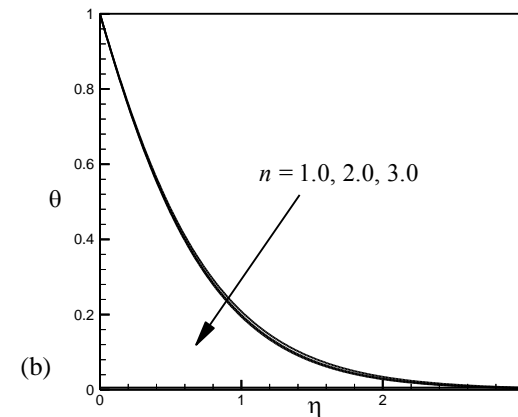
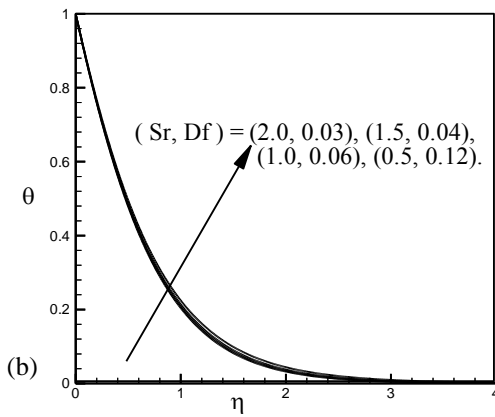
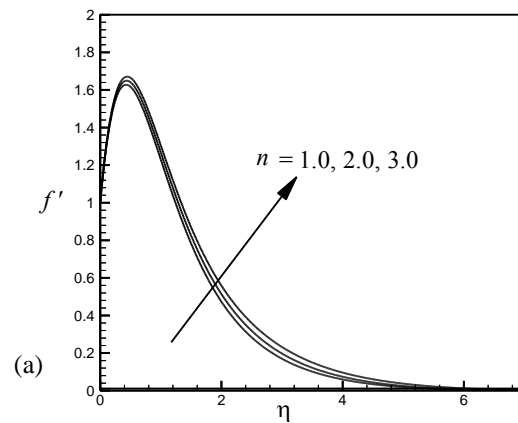
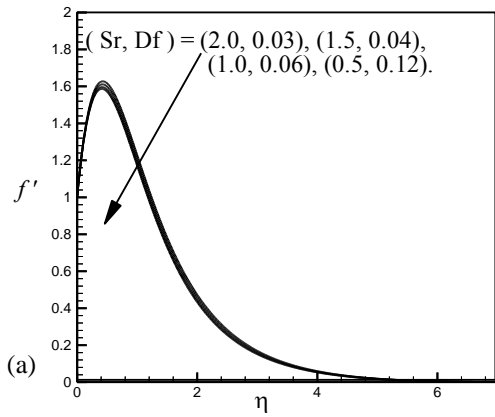


Fig.7: Variation of dimensionless (a) velocity, (b) temperature and (c) concentration profiles across the boundary layer for different values of  $(Sr, Df)$ .

Fig.8: Variation of dimensionless (a) velocity, (b) temperature and (c) concentration profiles across the boundary layer for different values of  $n$ .



TABLE-2: Effects of  $K$ ,  $Sr$  and  $Df$  on the local skin-friction coefficient ( $Cf_x$ ), local Nusselt number ( $Nu_x$ ) and local Sherwood number ( $Sh_x$ ) for  $g_s = 12$ ,  $g_c = 6$ ,  $Pr = 0.70$ ,  $Sc = 0.22$ ,  $r = 1.0$ ,  $f_w = 0.50$ ,  $Q = 0.50$ ,  $M = 0.50$ ,  $n = 1.0$  and  $\alpha = 45^\circ$ .

$K$	$Sr$	$Df$	$Cf_x$	$Nu_x$	$Sh_x$
-1.0	0.0	0.00	3.6288	1.3237	0.5009
0.0	0.0	0.00	3.4495	1.2927	0.7075
1.0	0.0	0.00	3.3422	1.2735	0.8611
2.0	0.0	0.00	3.2662	1.2600	0.9886
-1.0	0.5	0.12	3.7102	1.3315	0.4005
0.0	0.5	0.12	3.5403	1.2797	0.6176
1.0	0.5	0.12	3.4350	1.2506	0.7801
2.0	0.5	0.12	3.3598	1.2284	0.9146
-1.0	2.0	0.03	3.8905	1.3586	0.0698
0.0	2.0	0.03	3.6880	1.3245	0.3197
1.0	2.0	0.03	3.5544	1.3004	0.5088
2.0	2.0	0.03	3.4568	1.2822	0.6641

TABLE-3: Effects of  $K$  and  $n$  on the local skin-friction coefficient ( $Cf_x$ ), local Nusselt number ( $Nu_x$ ) and local Sherwood number ( $Sh_x$ ) for  $g_s = 12$ ,  $g_c = 6$ ,  $Pr = 0.70$ ,  $Sc = 0.22$ ,  $r = 1.0$ ,  $f_w = 0.50$ ,  $Q = 0.50$ ,  $Sr = 2.0$ ,  $Df = 0.03$ ,  $M = 0.50$  and  $\alpha = 45^\circ$ .

$K$	$n$	$Cf_x$	$Nu_x$	$Sh_x$
-1.0	1	3.8829	1.3692	0.0647
0.0	1	3.6797	1.3350	0.3149
1.0	1	3.5456	1.3107	0.5043
2.0	1	3.4475	1.2924	0.6599
-1.0	2	3.7772	1.3508	0.1479
0.0	2	3.6797	1.3350	0.3149
1.0	2	3.6070	1.3228	0.4495
2.0	2	3.5489	1.3129	0.5644
-1.0	3	3.7142	1.3405	0.2232
0.0	3	3.6797	1.3350	0.3149
1.0	3	3.6519	1.3304	0.3932
2.0	3	3.6284	1.3265	0.4624

#### 4. CONCLUSIONS

The influence of chemical reaction and heat generation/absorption on MHD free convection and mass transfer flow of a viscous, incompressible and electrically conducting fluid over an inclined stretching sheet with variable wall temperature and concentration is investigated numerically, by taking into account the Dufour and Soret effects. From the present numerical investigation it is observed that chemical reaction parameter  $K$ , the order of reaction  $n$ , heat generation/absorption parameter  $Q$  play a crucial role in the solutions. The presented analysis has also shown that the flow field is appreciably influenced by the

Dufour and Soret effects. Therefore we can conclude that for fluids with medium molecular weight ( $H_2$ , air), the Dufour and Soret effects should not be neglected.

#### REFERENCES

- [1] M. I. Char, "Heat and mass transfer in a hydro magnetic flow of the visco-elastic fluid over a stretching sheet," J. mathematical Analysis and Applications, Vol. 186(3), pp. 674-689, 1994
- [2] M. Acharya, L. P. Singh, G. C. Das, "Heat and mass transfer over an accelerating surface with heat source in the presence of suction and blowing," Int. J. Engng. Sci., Vol. 37, pp. 189-211, 1999.
- [3] S. K. Khan, M. S. Abel, R. M. Sonth, "Visco-elastic MHD flow; heat and mass transfer over a porous stretching sheet with dissipation of energy and stress work," Heat Mass Transfer, Vol. 40, pp.47-57, 2003.
- [4] E. Sanjayanand, S. K. Khan, "On heat and mass transfer in a visco-elastic boundary layer flow over an exponentially stretching sheet," Int. J. Thermal Sciences, vol. 45(8), pp.819-828, 2006.
- [5] J. R. Fan, J. M. Shi, X. Z. Xu, "Similarity solution of mixed convection with diffusion and chemical reaction over a horizontal moving plate," Acta Mechanica, Vol. 126, pp. 59-69, 1998.
- [6] H. S. Takhar, A. J. Chamkha, G. Nath, "Flow and mass transfer on a stretching sheet with a magnetic field and chemically reactive species," Int. J. Engng. Sci., Vol. 38 (12), pp. 1303-1314, 2000.
- [7] R. Muthucumaraswamy, P. Ganesan, "Effect of the chemical reaction and injection on flow characteristics in an unsteady upward motion of an isothermal plate," J. Appl. Mech. and Tech. Phys., Vol. 42(4), pp. 665-671, 2001.
- [8] A. J. Chamkha, "MHD flow of a uniformly stretched vertical permeable surface in the presence of heat generation/absorption and a chemical reaction," Int. Comm. Heat and Mass Transfer, Vol. 30(3), pp. 413-422, 2003.
- [9] R. Kandasamy, K. Periasamy, K. K. Sivagnana Prabhu, "Effects of chemical reaction, heat and mass transfer along a

- wedge with heat source and concentration in the presence of suction or injection,” *Int. J. Heat and Mass Transfer*, Vol. 48(7), pp. 1388-1394, 2005.
- [10] N. G. Kafoussias, E. M. Williams, “Thermal-diffusion and diffusion-thermo effects on mixed free-forced convective and mass transfer boundary layer flow with temperature dependent viscosity,” *Int. J. Engng. Sci.* Vol. 13, pp.1369-1384, 1995.
- [11] M. Anghel, H. S. Takhar, I. Pop, “Dufour and Soret effects on free-convection boundary layer over a vertical surface embedded in a porous medium,” *Studia Universitatis Babes-Bolyai, Mathematica*, Vol. XLV, pp.11-21, 2000.
- [12] N. T. Eldabe, A. G. El-Saka, A. Fouad, “Thermal-diffusion and diffusion-thermo effects on mixed free-forced convection and mass transfer boundary layer flow for non-Newtonian fluid with temperature dependent viscosity,” *Appl. Math. and Compt.*, Vol. 152, pp. 867-883, 2004.
- [13] A. M. Salem, “Thermal-diffusion and diffusion-thermo effects on convective heat and mass transfer in a visco-elastic fluid flow through a porous medium over a stretching sheet,” *Commun. in Numer. Meth in Engng.*, Vol. 22, pp.955-966, 2006.
- [14] M. S. Alam, M. M. Rahman, M. A. Samad, “Dufour and Soret effects on unsteady MHD free convection and mass transfer flow past a vertical porous plate in a porous medium,” *Non-linear Analysis: Modeling and Control*, Vol. 11(3), pp.217-226, 2006.
- [15] A. Postelnicu, “Influence of chemical reaction on heat and mass transfer by natural convection from vertical surfaces in porous media considering Soret and Dufour effects,” *Heat and Mass transfer*, Vol. 43, pp. 595-602, 2007.
- [16] P. R. Nachtsheim, P. Swigert, “Satisfaction of the asymptotic boundary conditions in numerical solution of the system of non-linear equations of boundary layer type,” *NASA TND-3004*, 1965.
- [17] H. I. Andersson, K. H. Bech, B. S. Dandapat, “Magnetohydrodynamic flow of a power law fluid over a stretching sheet,” *J. Non-Linear Mech.*, Vol 27, pp. 929-936, 1992.